Impact of Structure on Magnetic Coupling in CaV$_4$O$_9$

W. E. Pickett

Complex Systems Theory Branch, Naval Research Laboratory, Washington DC 20375
(Received 25 April 1997)

The strong corrugation of the V$_4$O$_5$ layer in the spin gap system CaV$_4$O$_9$ is examined for its impact on the exchange coupling constants between the spin-$\frac{1}{2}$ V ions. Local spin density calculations show that the V spin occupies a $d_{x^2-y^2}$ orbital ($\hat{x}$ and $\hat{y}$ are the V-V directions) that would have vanishing second order exchange coupling if the V$_4$O$_5$ layer were flat. The Kanamori-Goodenough superexchange rules, and the small calculated energy difference of ferromagnetic and antiferromagnetic alignments of spins for the real structure, indicate that second neighbor couplings dominate over nearest neighbor. This suggests two coupled $S = \frac{1}{2}$ *meta*plaquette systems, each tending toward singlet formation. [S0031-9007(97)03862-3]

From its vanishing susceptibility $\chi(T \to 0)$ [1] and related NMR properties [2], CaV$_4$O$_9$ is known to enter a quantum disordered phase with a spin gap. This behavior has stimulated theoretical investigation of the exchange couplings between the $S = \frac{1}{2}$ spins on the V lattice [3–9], using a Heisenberg model with nearest (nn, J_1) and next-nearest (nnn, J_2) exchange couplings. The $\frac{1}{5}$-depleted lattice [10] (described below) has been viewed as an array of square "plaquettes" of V ions tending toward singlet formation [3]. Isolated plaquettes have a singlet ground state; structural chemistry, however, suggests intra- and interplaquette nn V-V coupling (J_1 and J_1') should be similar, so the limit of isolated plaquettes is not realistic. We use the J_1, J_2, J_1', J_2' notation of Gelfand *et al.* [9].

Depletion alone does not destroy Néel order [5], and although competing interactions $J_1 \neq J_2$ lead to a quantum disordered ground state and $\chi(T) \to 0$, they do not account quantitatively for the $\chi(T)$ data [6,9]. Yet the "plaquette phase" of incipient singlets provides an attractive framework for accounting for the lack of magnetic ordering and the spin gap behavior. In this Letter we show that exchange interactions depend strongly on complications of the crystal structure, largely through the crystal field that gives an orbital character of the occupied V d spin orbital that is different than previously anticipated [3,4,8,11]. For this spin orbital, nnn exchange coupling exceeds nn coupling, unlike the assumptions made in previous work. We suggest here a picture of a two coupled *meta*plaquette systems that may preserve the tendency toward local singlet formation on each metaplaquette while enhancing frustrating couplings.

The crystal structure of CaV$_4$O$_9$ [10] has been idealized in most previous theoretical treatments to the consideration of flat VO layers with periodic V vacancies. The actual structure is much more interesting. The space group is simple tetragonal $P4/n$ (#85 in the International Tables), with $a = 8.333$ Å, $c = 5.008$ Å, and two formula units per cell. The low crystal symmetry is reflected in the fact that ten of the 15 internal structural parameters (for five sites) are not fixed by symmetry. Conceptually, one may start from a VO square lattice with cations and anions arranged as on a checkerboard. Each V ion along a V-O axis has an apical oxygen above (say) the layer, with V ions along neighboring V-O lines having their apical oxygen below the plane. V ions are removed in a pattern corresponding to a left-moving (or right-moving, giving the chiral partner) knight on a chessboard that lies at a 45° angle derived only from the V ions: from one V vacancy, go two V ions along a line of V ions, and one to the left to locate a neighboring vacancy. The resulting pattern, shown in Fig. 1, is a $\sqrt{5} \times \sqrt{5}$ enlargement with respect to the V sublattice, which is itself $\sqrt{2} \times \sqrt{2}$ larger than the VO square lattice. Ca ions arrange themselves either above or below the V vacancies.

Superimposed on this superstructure is a severe, cell-doubling corrugation of the plane, with V ions displaced alternately ± 0.625 Å perpendicular to the plane in the direction of their apical O ion. The entire structure is shown in Fig. 2. V ions, as well as apical ions (O2), remain equivalent by symmetry, but there are two other O sites. O1 sites are near (± 0.12 Å) the plane and are coordinated with three V ions, two on one plaquette and the third on a neighboring plaquette, all at 1.95–1.96 Å. O3 sites remain in the plane at positions at the plaquette center, and are fourfold coordinated with V ions at 2.04 Å. The compound can be written descriptively as [CaV$_4$O1$_4$-O2$_4$O3]$_2$. The V, O1, and O2 sites have no symmetry. The V ion lies within a tilted square pyramid of O ions ("square" of O1$_3$O3, with O2 apex), not far from the center of mass of the five O ions (Fig. 3). Each V$_4$ plaquette is boat-shaped, with two corner V ions up and the other two down. Due to the corrugation, the V-V-V angle that would be 180° for a plane is reduced to 130°.

We have applied the full potential linearized augmented plane wave (FLAPW) method [12,13] used in previous studies of magnetic transition metal oxide compounds. The sphere radii used in fixing the FLAPW basis were chosen to be 2.0, 2.0, 1.60, 1.45, and 1.60 a.u. for Ca, V, O1, O2, and O3, respectively. Local orbitals were added to the basis set for extra flexibility and to allow semicore states to be treated within the same energy window as the band states. For the V atoms, s, p, and d local orbitals
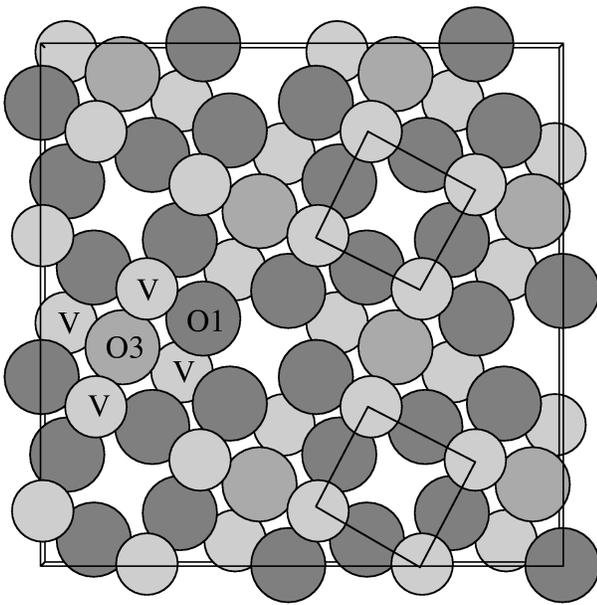
FIG. 1. Top view of the V_4O_5 layer, with Ca and O2 atoms not displayed. A plaquette of V ions is labeled by "V." Two metaplaquettes, formed by the V ions above the layer, are shown by the solid lines.

were used, while for Ca and the O atoms s and p local orbitals were added. The plane wave cutoff corresponded to an energy of 19 Ry. The total basis set size is 3350 LAPW's and local orbitals.

An initial calculation without spin polarization found the O $2p$ states to be centered 6–7 eV below the center of the V $3d$ bands, and separated from them by a gap of 2 eV. The lowest Ca-derived bands arise from the $3d$ states, but lie above the V d bands and are inactive. The Fermi level E_F lies low in the V d bands, corresponding to a d^1 configuration. Thus the conventional ionic picture is well respected in this compound.
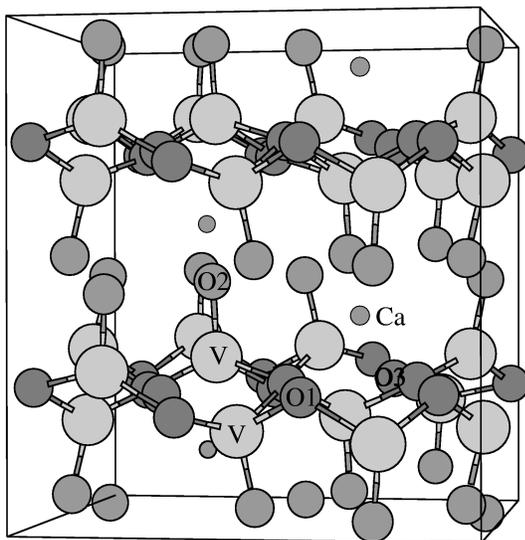
FIG. 2. Structure of CaV_4O_9, from Bouloux and Galy [10], illustrating the severe corrugation of the V-O layer. Unit cells in two successive layers are shown.
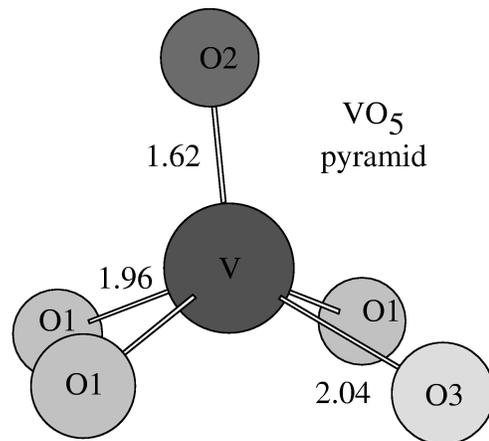
FIG. 3. Side view of the VO_5 "pyramid." The V ion actually lies above the center of mass of the five O ions. V-O bond lengths (Å) are shown. The three V-O1 lengths are inequivalent but nearly equal.

To interrogate magnetic interactions, ferromagnetic (FM) and antiferromagnetic (AFM) alignments of the V moments were studied. For FM ordering, an insulating state is obtained, as shown in Fig. 4, so the moment obtained is precisely $1\mu_B$ per V. An insulating result was not anticipated from the nonpolarized calculation: there was no gap in the d bands, so a rigid Stoner splitting of majority and minority bands would leave a metallic result. The lowest lying V d orbital in the majority bands, which we show below to be the $d_{x^2-y^2}$ orbital, upon polarization becomes separated from the remaining four $3d$ orbitals, due to an exchange splitting Δ_{ex} that is strongly orbital dependent. $\Delta_{ex}(d_{x^2-y^2}) \approx 1.3$ eV is an unusually large value (LSDA exchange forces usually are less than 1 eV/μ_B), reflecting a weakly hybridized (and therefore more confined) $d_{x^2-y^2}$ orbital. Δ_{ex} is only about 0.6 eV in the center of the d bands and decreases to 0.4 eV at the top. The calculated gap in the majority bands is 0.7 eV, and the gap between occupied majority and unoccupied
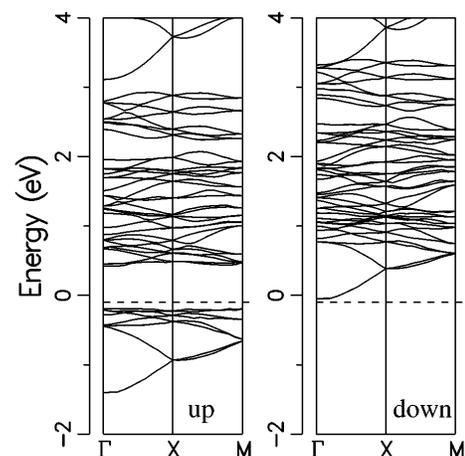
FIG. 4. Majority (left) and minority (right) bands along high symmetry directions for FM CaV_4O_9. The majority $d_{x^2-y^2}$ states (one for each V ion) are disconnected from other d states, leading to an insulating result.

minority bands is of the order of 0.1 eV. Correlations effects may increase the gap, perhaps substantially.

The spin density for this FM state, shown in Fig. 5, is clearly that due to occupation of a single spin-orbital of the V $d_{x^2-y^2}$ character, where $\hat{x}$ and $\hat{y}$ refer to the lines of V ions. Because of the low V ion site symmetry, the lobes do not point precisely in the direction of neighboring V ions nor lie exactly in the crystallographic $\hat{x} - \hat{y}$ plane, but these misalignments are only a few degrees. These spin orbitals are nonbonding with respect to the neighboring O ions, a point we return to below. This occupied orbital is not of the type (d_{xy}, d_{yz}, d_{xz}) anticipated in previous work [4,8], or used by Marini and Khomskii in orbital ordering arguments (d_{xz} or d_{yz}) [11]. Note that this orientation is actually determined by the crystal field rather than any orbital ordering instability, and is unrelated (at least for this narrow band system) to the FM order.

The chosen AFM order was of the Néel type; each V spin is antiparallel to its two neighbors on a plaquette and to the neighbor on the next plaquette. This type of order breaks inversion symmetry, and all V ions on one side of the (idealized V-O) plane have the same spin direction. The resulting state is also insulating, and as expected the occupied bandwidth is smaller (20%) than for FM alignment. The AFM state is lower in energy than the FM alignment by only 4.6 meV/V. In terms of a classical Heisenberg model [14] with interactions J_1, J_1', J_2, J_2', the nnn couplings J_2, J_2' cancel, giving the difference $2(J_1 + \frac{1}{2}J_1')S^2 = 4.6$ meV, which becomes $\frac{2}{3}J_1 + \frac{1}{3}J_1' = 6$ meV $\rightarrow 70$ K. Estimates else-
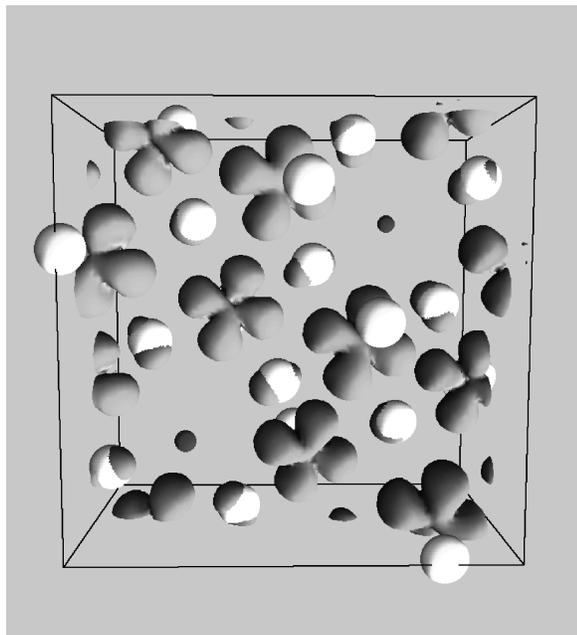
FIG. 5. Top view of an isocontour of the spin density of FM CaV$_4$O$_9$ (truncated at the cell boundaries), illustrating the occupied $d_{x^2-y^2}$ V^{4+} spin orbital. The white spheres indicate oxygen sites, small dark spheres indicate Ca ions.

where suggest that J_2' should be 200 ± 20 K to account for the spin gap [15] and for the excitation spectrum [16].

The effective V $d_{x^2-y^2} - d_{x^2-y^2}$ transfer integrals are mediated *via* virtual hopping processes through the intervening O ions, with amplitudes $t_{dp\sigma}$ and $t_{dp\pi}$, and perhaps through direct V-V coupling. In the idealized V$_4$O$_5$ parent layer, the O ions lie at 45° angles to the V-V nn direction. In terms of hopping processes, the nnn V ion is no more distant that the nn V ion. According to the Goodenough-Kanamori (GK) rules [17], the hopping amplitudes depend strongly both on the symmetry of the d and p orbitals involved and on the V-O-V angles. The first point to note is that this spin orbital is orthogonal (except for the $\phi \approx 5°$ rotation) to the O p_σ orbital; hence, the coupling must proceed through the p_π orbital. This coupling involves only the $t_{dp\pi}$, which may be 2-3 times smaller than $t_{dp\sigma}$. The p_π orbital couples to the $d_{x^2-y^2}$ orbital on the nnn V (again via $t_{dp\pi}$). The p_π orbital, however, is *orthogonal* to the $d_{x^2-y^2}$ orbital on the nn V (with respect to which it is a p_σ orbital). Thus the usual second order nn V superexchange coupling vanishes in the idealized layer for this spin orbital.

Because of the symmetry lowering distortions, this vanishing is incomplete, and the surviving coupling may be larger than higher order effects involving polarization of the O ion [17]. $pd\sigma$ hopping is allowed as $t_{dp\sigma} \sin \phi$ and $pd\pi$ hopping is reduced to $t_{dp\pi} \cos \phi$. The couplings become

$$J_1, J_1' \propto 2(t_{dp\pi} \cos \phi \, t_{dp\sigma} \sin \phi)^2/(\varepsilon_d - \varepsilon_p)^3, \quad (1)$$

$$J_2, J_2' \propto (t_{dp\pi}^2 \cos^2 \phi)^2/(\varepsilon_d - \varepsilon_p)^3, \quad (2)$$

where the factor of two arises from the two paths, and $\varepsilon_d - \varepsilon_p \approx 3$–4 eV is the energy separation between V d and O p states. Since $\sin \phi \approx 0.1$, a rough estimation gives $J_2/J_1 \approx \frac{1}{2}(t_{dp\pi}/t_{dp\sigma})^2 \cot^2 \phi \approx \frac{1}{2} \times \frac{1}{3^2} \times 100 \approx 5$.

This already rough estimate will be altered further by the structural corrugations. nn V ions, which differ in z coordinate by 1.25 Å, are connected along two V-O-V paths, whose contributions add. For nnn V ions, which are at the same height, there is a single path. Within a plaquette, the angles for nn V ions are $\phi_{1a} = 100°$ (V-O1-V) and $\phi_{1b} = 95°$ (V-O3-V), and is $\phi_2 = 144°$ (V-O3-V) across the diagonal. Between plaquettes, nn V are connected by two identical $\phi_{1a}' = \phi_{1b}' = 100°$ angles (V-O1-V), while the diagonal nnn angle is $\phi_2' = 130°$ (V-O1-V). These angular variations, coupled with the facts that the O ions are not coplanar with the lobes of the $d_{x^2-y^2}$ spin orbital, that O1 and O3 are distinct, and that direct V-V exchange may not be negligible, make it difficult to make GK estimates of relative values of exchange couplings.

The two distinct direct V-V separations are 3.00 ± 0.01 Å, which can be compared to the bondlength in V metal of 2.73 Å. This difference of less than 10% suggests that direct V-V hopping might be appreciable. The less extended nature of the V^{4+} orbitals compared to neutral V orbitals will reduce the overlap, however. Since nn

V ions do not lie in the plane of the $d_{x^2-y^2}$ orbital, the orbital must be rotated by $\theta = \sin^{-1}(\frac{1.25}{3.00}) = 25°$ on both atoms before the overlap can be expressed in terms of the usual $t_{dd\sigma}, t_{dd\pi}, t_{dd\delta}$ hopping amplitudes. Neglecting the latter two, which at this distance should be much smaller than $t_{dd\sigma}$, the effective hopping between the nonaligned $d_{x^2-y^2}$ spin orbitals will go as $t_{dd\sigma}\cos^2\theta$, a reduction by $\cos^2\theta \approx 0.8$.

It is not a straightforward matter to determine the relative importance of direct V-V hopping and V-O-V mixing that gives the dispersion pictured in Fig. 4. The effect on the d bandwidth of the V-O-V coupling was probed by moving the O2 ions from $\frac{z}{c} = 0.939$ to $\frac{z}{c} = 0.75$. This distortion brings the O2 ion nearer one V, but much farther from the other (2.6 Å), essentially eliminated V-O1-V coupling of neighboring plaquettes. The resulting occupied d bandwidth of $W_d = 0.4$ eV, compared to 1.3 eV for the real structure, can be ascribed to direct V-V coupling. This result suggests that coupling through the O1 ions is responsible for roughly $\frac{2}{3}$ of the bandwidth, with direct V-V interactions providing the remaining $\frac{1}{3}$; i.e., direct V-V coupling is not negligible. This complexity arises specifically from the fact that the spin-orbital is $d_{x^2-y^2}$ character, which greatly hinders coupling to O ions and maximizes V-V interaction. Using a coordination number $z_c = 3$, the V-V bandwidth translates to a hopping amplitude $t_{dd\sigma} = W_d/(2z_c\cos^2\theta) = 80$ meV.

The hybridization leading to magnetic coupling is reflected in the spin density distribution on O ions neighboring V. The primary feature, in both FM and AFM alignments studied, is an *antiparallel* polarization of the apical O2 by roughly 0.2 μ_B. This O2 ion, however, is not involved in exchange coupling. The O1 ions have moments about $\frac{1}{3}$ as large, aligned parallel, while the O3 ion's moment is even smaller (zero by symmetry for AFM case). Thus the O1 site should be more active in the exchange coupling process than is the O3 site.

This observation leads to one particularly interesting difference between the original plaquette system and (either one of) the metaplaquette systems. As was noted in the introduction, V-O-V couplings within a plaquette, or between neighboring plaquettes, are very similar from the structural chemistry point of view. The metaplaquette system is different; intrametaplaquette coupling (J_2') proceeds through the O1 site, while intermetaplaquette coupling (J_2) proceeds through the O3 site. Not only is the V-O3 distance 4% longer than the V-O1 distance (Fig. 3) resulting in weaker coupling, but the environments are different and the LSD calculation indicates substantially less hybridization through the O3 site, as reflected in the much lower induced O3 spin density. This O1-O3 site distinction suggests $J_2' > J_2$ and provides a mechanism whereby the tendency to form singlets on each metapla-

quette is not disrupted by equally strong intermetaplaquette coupling. Moreover, there is no coupling across the diagonal of the metaplaquette to frustrate singlet formation, as was the case for the plaquettes.

These results—the occupied spin orbital of $d_{x^2-y^2}$ character, $J_2' \approx 200$ K and $J_2' \gtrsim J_2$, a small FM-AFM energy difference indicating relatively small values of J_1 and J_1'—suggest a system comprised of two coupled metaplaquette arrays. Each metaplaquette is comprised solely of V ions either above the plane, or below the plane (the upper metaplaquette is highlighted in Fig. 1). Although we have no direct information at present, structural considerations suggest that J_2 is comparable to, but smaller than, J_2', i.e., $J_2' > J_2 > J_1 \approx J_1'$. Then each metaplaquette system is coupled more strongly within its own metaplaquette system (J_2) than to the other metaplaquette system (J_1, J_1'). This coupled two metaplaquette system may provide a realistic way to interpret the spin gap behavior. As already pointed out by Gelfand and Singh [15], this picture predicts that the minimum in the triplet excitation spectrum occurs at the Brillouin zone center, and this feature was observed recently by Kodama *et al.* [16].

I thank R. R. P. Singh for stimulating my interest in this compound, and acknowledge helpful comments from C. S. Hellberg. This work was supported in part by the Office of Naval Research. Computation was done at the Arctic Region Supercomputing Center and at the DoD Major Shared Resourse Center at NAVOCEANO.

[1] S. Taniguchi *et al.,* J. Phys. Soc. Jpn. **64**, 2758 (1995).
[2] T. Ohama *et al.,* J. Phys. Soc. Jpn. **66**, 23 (1997).
[3] K. Ueda *et al.,* Phys. Rev. Lett. **76**, 1932 (1996).
[4] K. Sano and K. Takano, J. Phys. Soc. Jpn. **65**, 46 (1996).
[5] M. Troyer *et al.,* Phys. Rev. Lett. **76**, 3822 (1996).
[6] O. A. Staryk *et al.,* Phys. Rev. Lett. **77**, 2558 (1996).
[7] M. Albrecht *et al.,* Phys. Rev. B **54**, 15 856 (1996).
[8] N. Katoh and M. Imada, J. Phys. Soc. Jpn. **64**, 4105 (1995).
[9] M. P. Gelfand *et al.,* Phys. Rev. Lett. **77**, 2794 (1996).
[10] J.-C. Bouloux and J. Galy, Acta Crystallog. B **29**, 1335 (1973).
[11] S. Marini and D. I. Khomskii, Report No. cond-mat/9703130.
[12] S. H. Wei and H. Krakauer, Phys. Rev. Lett. **55**, 1200 (1985); D. J. Singh, Phys. Rev. B **43**, 6388 (1991).
[13] D. J. Singh, *Planewaves, Pseudopotentials, and the LAPW Method* (Kluwer Academic, Boston, 1994).
[14] Y. Fukumoto, J. Phys. Soc. Jpn. (1997, to be published).
[15] M. P. Gelfand and R. R. P. Singh, Report No. cond-mat/9705122.
[16] K. Kodama *et al.,* J. Phys. Soc. Jpn. **66**, 793 (1997).
[17] J. B. Goodenough, *Magnetism and the Chemical Bond* (Wiley, New York, 1963), Chap. IIIC.